JOURNAL OF CATALYSIS 138, 38–54 (1992)

The Adsorption/Impregnation of Pd(II) Cations on Alumina, Silica, and Their Composite Oxides

J. A. SCHWARZ,[1] C. T. UGBOR, AND R. ZHANG[2]

Department of Chemical Engineering and Materials Science, Syracuse University, Syracuse, New York 13244-1190

Received January 15, 1992; revised June 4, 1992

Two models are proposed to evaluate the electric charge structure of alumina on silica and silica on alumina composite oxides. The data for these models have been determined at pH and ionic strength conditions identical to those employed during Pd(II) cation adsorption/impregnation. From these models we determine the inventory of negative charge on each support. The model, which considers that both the geometrical and charge structure of the oxide system can be represented as a simple additive contribution of each of the pure phases (i.e., Al_2O_3 and SiO_2), is shown to be consistent with the strongly adsorbed $Pd(NH_3)_4^{2+}$ adsorbed amount determined from adsorption isotherm measurements. © 1992 Academic Press, Inc.

INTRODUCTION

In many cases, supported metal oxide catalysts are prepared by impregnation of the oxide carrier with an aqueous solution of a metal salt. The adsorption of the metal ions is influenced by intrinsic properties of the support, and any modeling of ion adsorption requires the determination of equilibrium constants for the surface ionization reactions germane to the support. These data, on the basis of any number of models for the electrical double layer, yield the pH-dependent surface charge development on the oxide. Successful modeling of this adsorption phenomenon also requires information on the pH-dependent aqueous phase speciation of the precursor ion *and* a suitable model to describe the adsorption/exchange reaction (*1, 2*).

Numerous proposals exist in the literature for describing the surface charge development on oxides. Included in these are the constant capacitance model (*3*), the diffuse layer model (*4*), the Stern model (*5*), and the triple-layer model (*6*). They differ inter alia by the manner in which they depict the electric double layer. Our earlier work has demonstrated that a simple diffuse layer model accurately predicts the adsorbed amounts of ionic solutes (*7*). This model's simplicity lies in the fact that adsorption occurs on one surface plane, thus eliminating any assumption of multiple planes for adsorption at the surface and the additional fitting parameters associated with them.

In recent studies from our laboratory, we have confirmed earlier assertions that Pd(II) ions conform to an electrostatically driven (adsorption) interaction with common supports such as SiO_2 or Al_2O_3 (*8*). Pd(II) ions derived from $PdCl_2$ are anionic in the presence of excess chloride ions and cationic in the presence of excess ammonium ions. Over a wide pH range, various complex species with chloride and/or ammonium ligands exist with electric charges between -2 and 2. At pH values <2, stable species of $PdCl_4^{2-}$ are formed; at pH values >8, stable species of $Pd(NH_3)_4^{2+}$ are formed (*9*).

Brunelle has proposed an adsorption model which emphasizes the electrostatic aspects of the adsorption process (*1*). This

[1] To whom correspondence should be addressed.
[2] Scientific Committee of Lanzhou, P.R. China.

0021-9517/92 $5.00
Copyright © 1992 by Academic Press, Inc.
All rights of reproduction in any form reserved.

model is reasonably complete. Chemical and physical interactions are considered together in calculating surface–solution equilibria. In this work, we use a simple diffuse layer model for the electrical double layer and assume all ion transfer to the support is controlled by electrostatic effects. On the basis of this and the above, it is reasonable to assume that the elements necessary to predict adsorption/impregnation of Pd(II) compounds onto Al_2O_3 and/or SiO_2 are available.

Recent work from our laboratory, using the above assumptions, has demonstrated that Pd(II) cationic and anionic complexes adsorbed amounts could be reasonably predicted as a function of the extent of dehydration of a laboratory prepared aluminium oxide (*10*). We also found, following the same electrostatic model, the partitioning of Pd(II) cations between Al_2O_3, SiO_2, and a 10% Al_2O_3 on SiO_2 composite oxide to be directly and predictably related to the impregnant pH (*8*).

Composite oxides represent a relatively new class of mixed oxide supports that have potentially unique properties as carriers for catalytic metals (*11*). We have studied the amphoteric properties of several composite oxide systems with the objective of determining their surface charge development in aqueous environments (*12, 13*). We find that the pH at which the net charge on the surface of a composite oxide is zero lies between the values characteristic of each of the pure oxides. This point of zero charge (pzc) is a useful parameter for modeling the "geometrical structure" of composite oxides. The results of such modeling have provided a measure of the surface area of the second-phase oxide component (*12*). Here, the term surface area is taken to mean the "apparent" area seen by electrolyte ions that conform to the site-binding model.

With these principles in place, we proposed that a selective metal–support exchange or pH directed adsorption/impregnation could be achieved using composite oxides (*11*). This proposal exploits the differences in the charge on each oxide surface at given pHs between the pH's spanning the pzc of each of the pure oxides. While this simple idea has proven to have merit, it is not sufficient in itself. The pzc is related to the two intrinsic acidity constants by (*14*)

$$\text{pzc} = \frac{\text{p}K1 + \text{p}K2}{2},$$

and it can be measured directly. Another parameter, which must be determined indirectly, is the difference in the two pK values, i.e., (p$K2$ − p$K1$). This difference, denoted as DPK, has been shown to also be an important parameter for determining the pH-dependent distribution of ionizable surface groups (*7*).

The value of the DPK is a measure of the fraction of charged sites when the pH is equal to the pzc. In other words, when the oxide is maintained at a pH = pzc although its net charge is zero, there exists some inventory of positive, negative, and neutral surface groups. Now, in relation to the selective metal–support exchange hypothesis, what this means is conditions may be such that ion adsorption on one phase of a composite oxide might be favorable based on pzc considerations, but this does not preclude adsorption onto existing charged sites of the second phase.

Since each phase of a composite oxide offers adsorption sites for catalytic precursor ions, a semiquantitative model of the distribution of charge density on the composite oxide surface is needed. The objective of this work is to demonstrate that such a model can be constructed based on appropriately weighting the charge density present on the pure oxides at the prevailing pH (and ionic strength) of the impregnant. The adsorption/impregnation of Pd(II) cations $[Pd(NH_3)_4^{2+}]$ onto composite oxides of SiO_2 on Al_2O_3 and Al_2O_3 on SiO_2 was studied at a pH = 10.6 and electrolyte ionic strength of 0.07 *M*. The charge density, under these conditions, of each oxide weighted by the "apparent" surface area of that phase in the composite was used to evaluate the number

of positive, negative, and neutral sites on the composite oxide. We find that this approach provides a semiquantitative measure of the equilibrum adsorption capacity of Pd(II) cations on this oxide system.

From a practical point of view, there is considerable interest in optimizing the performance of catalyst systems by proper regulation of their preparative procedures. A number of systems offer the possibility for design by the selective metal-support exchange hypothesis. For example, we ask rhetorically, can Co and/or Ni be selectively mounted on a specific component of a WO_3/Al_2O_3 or MoO_3/Al_2O_3, mixed oxide *and* if so, are there any catalytic advantages? Other systems might include $Rh//CeO_2/Al_2O_3$, extensively studied for its application in automotive pollution control and $V_2O_5//TiO_2/SiO_2$, the selective reduction catalyst (SCR) for NO_x abatement.

EXPERIMENTAL

Procedures for the preparation of the pure oxides (alumina and silica) composite oxides (alumina on silica and silica on alumina) as well as the methods employed in their characterization are presented in this section.

MATERIALS

A. Alumina

The aluminium oxide support used in this work was derived from aluminum isopropoxide (98+% pure) supplied by Aldrich. An amount of aluminum isopropoxide to obtain 100 g of oxide was weighed and the solid compound was crushed to particle sizes below 40 mesh. The resulting fine powder was dispersed in an excess amount of deionized water by continuous stirring of the mixture. The heat of solution that developed caused the mixture to form a white paste. The sample was then placed into an oven under air circulation at 393 K. Hydrolysis and gelation required 15 h. The sample was crushed to between 40 and 80 mesh particle size with an average particle size of approximately 0.225 mm. It was then calcined at 873 K for 24 h in air.

B. Silica

Silica was derived from tetraethylorthosilicate (98% pure supplied by Aldrich). For the preparation of approximately 100 g of SiO_2, 366 ml of tetraethylorthosilicate, 170 ml of ethanol (Absolute-200 proof supplied by AAPER Alcohol Chemical Company), and 400 ml of deionized water were put into a 1000-ml beaker. This mixture was continuously stirred for 18 h, after which time a clear homogeneous solution was obtained. The temperature of this solution was gradually increased with reduced stirring rate until the gelation point of the solution. The gel was then broken into smaller particle sizes by stirring with a glass rod and transferred to a drying oven (Labline, Cat. No. 3505) and maintained at 383 K with air circulation to dry overnight. The dried sample was reduced to particle sizes between 40 and 80 mesh. The sample was then calcined at 873 K for 24 h in air.

C. Physical Mixtures

Physical mixtures of the two oxides were prepared with the respective masses of each pure phase required to give a specified composition. These were prepared starting from 0% mass content of Al_2O_3 (100% SiO_2) to 100% mass content of Al_2O_3 (0% SiO_2). After mixing the appropriate proporton by mass, these mixtures were given a manual, thorough shaking, to assure homogeneity before use.

D. Composite—Alumina on Silica

Deionized water in excess of that needed to fill the pores of silica (0.5 ml/g pore volume by water titration) was employed in the hydrolysis of aluminum isopropoxide used in the preparation of the desired weight loadings of alumina on calculated amounts of silica. The aluminum isopropoxide was stirred in water until the heat of solution was released (i.e., until the formation of the white paste), then a calculated amount of

silica was introduced with continuous stirring. It was observed that the heat generated by the system increased with the introduction of silica. The resulting composite was dried in the oven at 393 K overnight and later calcined at 873 K for 24 h in air. It was cooled to room temperature in the furnace and later transferred into plastic containers for storage.

E. Composite—Silica on Alumina

The volume of tetraethylorthosilicate required to give a certain loading was determined. The difference between this volume and the volume of liquid needed in a small excess of the pore volume of Al_2O_3 (1.2 ml/g water titration) was made up with ethanol and water in the ratio of 0.425 : 1 by volume. This mixture was stirred continuously for 18 h, at which time the needed mass of Al_2O_3 was introduced while mechanically stirring with a glass rod. The sample was then put in the oven to dry overnight. The composite oxide was later calcined in the furnace at 873 K for 24 h.

F. Palladium Complex

Palladium chloride (99.9% pure, Lot No. F11A33) supplied under the metal loan program of Johnson Matthey Company was used in this work. The molar ratio of palladium chloride to 12 *M* HCl (Fisher Scientific Co., Lot No. 732051) varied between 0.023 and 0.029 *M*, respectively. This gave a palladium chloride solution at pH ~ 1.50 and ionic strength of 0.07 *M*. The minimum amount of ammonium hydroxide (Aldrich Chemical Co.) was introduced into the palladium chloride solution to form the cationic complex of this metal ion. It was observed that the color of the final solution was dependent on the rate of introduction of ammonium hydroxide. A fast rate with continuous stirring resulted in a homogeneously clear liquid system. On the other hand, a delayed or slow rate of introduction would result in a brownish solution or even a magenta color with precipitates. The brownish solution was not convertible to the clear solution. For uniformity in the preparation of the metal complex, conditions were maintained such that the homogeneously clear solution was formed each time.

PROCEDURES

A. BET Surface Area

A Quantasorb sorption apparatus was used to obtain the BET surface area at liquid-nitrogen temperature for all the samples used. The single-point BET method was employed using a 15% nitrogen in helium gas mixture (ultrahigh purity grade, minimum purity of 99.999% supplied by Linde Gas Co.). The samples were pretreated by heating to 393 K overnight before all measurements.

B. Mass Titration

Sodium nitrate solution with ionic strength of 0.1 *M* was found adequate in buffering the metal oxide suspension in deionized water for point of zero charge (pzc) determination. The method used is described elsewhere (*15*). Briefly, for each oxide, seven plastic bottles were used with typical oxide to sodium nitrate solution mass percents of 0, 1.5, 2.5, 3.4, 5, 7, and 9.1. The containers were sealed and placed on a Wrist Action shaker (Burrell Corp., Model 75) for 24 h. A 1-day period was sufficient time to attain equilibration of the metal oxide suspension system. At the end of this period, a Corning pH meter (Model No. 145) was used to measure the pH of the suspension. The meter was calibrated at pH = 4 and pH = 10 using certified buffer solutions (Fisher Scentific Co.).

C. Potentiometric Titration

Sodium nitrate solutions of ionic strengths 0.001, 0.01, and 0.1 *M* were prepared. Three sets of nine 25-ml plastic bottles were used; each held 20 ml solution at the three ionic strengths. Into each of these bottles, 200 mg of the metal oxide to be measured (viz. Al_2O_3, 7% Al_2O_3, 3% Al_2O_3, 3% SiO_2, 7% SiO_2, 10% SiO_2, and SiO_2) was placed. Four of the bottles that belong to

each ionic strength were assigned to hold 20 drops, 15 drops, 10 drops, and 5 drops of 0.1 *N* HNO_3 (Fisher Scientific Co., Lot No. 890078-24). Four other bottles from each ionic strength held the same distribution of drops of 0.1 *N* NaOH solution (Fisher, Lot No. 862217-24). The remainder of the bottles held no acid or base. The masses of these drops of acid to base were recorded for subsequent analysis.

Blank experimental runs were carried out at the same ionic strengths of solution but without the metal oxide in suspension. The blank run was used to remove the background adsorption of ions and in determining the quantity of potential determining ions that were consumed by the support (metal oxide).

D. Adsorption/Impregnation

The Pd cation was chosen as the adsorbate; its speciation at pH > 8 is $Pd(NH_3)_4^{2+}$. The adsorption conditions were designed so that constant ratios of surface area of solids to the volumes of solution were maintained (6.5×10^4 cm^{-1}). An amount of impregnant (50 ml) was pipetted into a 250-ml beaker maintained at a pH of 10.6. Also, a small amount of this solution was pipetted into a 100-ml flat-bottom flask for later measurement. The necessary amount of the porous metal oxide was weighed out. A burette containing ammonium hydroxide solution was used for maintaining the pH = 10.6 during the adsorption experiment. The amount of added base was small enough that the ionic strength was not affected. After the porous metal oxide was introduced into the solution of the active ingredient, the system was continually agitated by hand for 1 h. Then both the solid and the liquid phases were sampled. The sampled solid was washed several times (*6*) to remove all pore-filling and nonelectrostatically held components of the active ingredient on the support. These washings were saved for analysis using an atomic absorption spectrophotometer (Model No. 2380) supplied by Perkin–Elmer.

TABLE 1

BET Surface Area for the Alumina–Silica Pure and Composite Oxide System

Support	Result (m^2/g)
Al_2O_3	174
3% SiO_2	184
7% SiO_2	185
10% SiO_2	187
20% SiO_2	260
80% Al_2O_3	234
60% Al_2O_3	376
40% Al_2O_3	487
20% Al_2O_3	499
10% Al_2O_3	550
7% Al_2O_3	551
3% Al_2O_3	621
SiO_2	648

E. AA Measurements

Palladium AA calibration experiments were conducted using a standard solution containing 5-wt% HCl supplied by Aldrich (Lot No. 04201LW). Aliquots of samples extracted during adsorption/impregnation experiments were diluted to fall into the linear range of the calibration. Fourteen readings of each sample were taken; the lowest and highest were disregarded and the remainder used to determine an average concentration.

RESULTS

BET Surface Areas

The BET surface areas of the pure supports as well as 11 composite oxides are given in Table 1. The data for the composites were obtained for both Al_2O_3 and SiO_2 acting as the second-phase oxide. The surface area for SiO_2 is more than three times that of Al_2O_3. Estimates of the error for such high-surface-area supports are within ±5%. The effect of increasing the concentration of second-phase oxide appears to be different for Al_2O_3 compared to SiO_2. In general, we would expect the effect of introducing a second-phase precursor would be to have

it fill/block porosity of the primary phase. Thus, we should see a decrease in surface area. Indeed, this is what is found for the case of Al_2O_3 on SiO_2. On the other hand, for SiO_2 on alumina, the BET areas are greater than that of Al_2O_3 and furthermore show substantial increase even at a loading of 20% SiO_2/Al_2O_3. One possible explanation for this effect is related to the properties of the primary phases, specifically their pore volume. The pore volume of Al_2O_3 is more than 100% that of SiO_2 (cf. Al_2O_3 1.20 cc vs SiO_2 0.5 cc). During impregnation of the second-phase precursors to form the composites, the aluminum compound could simply fill/block the exterior of the SiO_2 pore structure which after activation would result in restricting N_2 penetration into some of its pores and a concomitant loss in BET area. On the other hand, when the silica precursor is loaded on the Al_2O_3 support, the large pore volume could accommodate the silicon compound on the walls in the external region of the Al_2O_3 pores. Recall, the second-phase compound (SiO_2) is the same compound used to make pure SiO_2, which itself has a high surface area. Assuming in the dispersed phase it contributes a surface area proportional to its pure phase value, the data in Table 1 should show an increase in BET with increasing SiO_2 concentration; indeed they do.

The data presented in Table 1 can be viewed from another perspective. If all samples are treated equivalently, we find the BET surface areas of the composites are well represented (correlation coefficient 0.99) as a mass-weighted average of the BET surface areas of the pure components. It is important to note, however, each of the viewpoints presented above consider the properties of this oxide system from the point of view of a gaseous probe (N_2). Shortly, we present the results obtained when the *probe* is aqueous; the results in this case might be more relevant to the characterization of these samples in the context of this study.

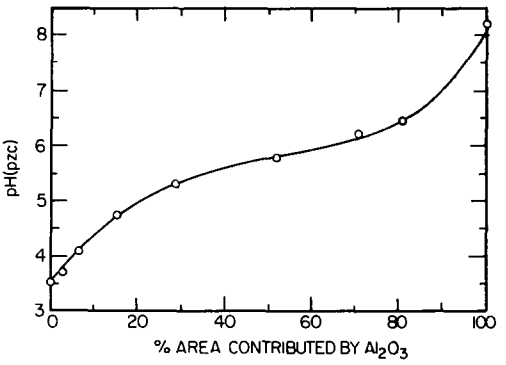

FIG. 1. The pH_{pzc} of physical mixtures of Al_2O_3 and SiO_2 vs the % area contributed by Al_2O_3. Error in pH measurement ±0.05. The solid line is drawn to connect points.

POINT OF ZERO CHARGE

Physical Mixtures

Mass titration was used to determine the pzc of the physical mixtures. This method provides a reasonable estimate of the pzc, it is convenient, and it is fast. Figure 1 shows the pzc of the physical mixtures plotted against the area (BET) contributed by a reference support. Here we use Al_2O_3. The nonlinear behavior has been seen before (*13*); qualitatively, this behavior can be explained by the fact that the amphoteric properties of the hydroxyl inventories on Al_2O_3 and SiO_2 are not the same. However, we note that at low concentration of either dopant, the pzc varies linearly with % contributed area. These data are used as a calibration curve to determine the structure of the composite oxides using a model presented by us earlier (*12, 13*).

Composite Oxides

Both mass titration and potentiometric titration were used to determine the pzc of this oxide family. Potentiometric titration data were required for calculating the surface charge by a model which we designate the common hydroxyl model. This model is discussed in the next section. Mass titration was used as a check on the approximate pzc

TABLE 2

pH pzc for the Alumina–Silica Pure and Composite Oxide System

Support	pH pzc (mass titration)	pH pzc (potentiometric titration)
Al_2O_3	8.2	8.52
1% SiO_2	7.81	—
3% SiO_2	—	7.29
5% SiO_2	7.07	—
7% SiO_2	6.5	6.39
10% SiO_2	5.75	5.37
80% Al_2O_3	6.52	—
60% Al_2O_3	5.71	—
40% Al_2O_3	5.16	—
20% Al_2O_3	4.75	—
7% Al_2O_3	3.87	3.94
3% Al_2O_3	3.64	3.79
1% Al_2O_3	3.57	—
SiO_2	3.52	3.2

of each support when a common intersection point at the pH = pzc was not "clearly visible" from the potentiometric titration data. Table 2 gives the results from each method. Very reasonable agreement occurs regardless of the method used, *and* we find that intermediate compositions always have pzc's that lie between the two pure supports.

Here, as in the case of the BET measurements, we ask if it is more or less appropriate to consider this oxide system as a unit or to differentiate between them based on the primary phase (SiO_2 or Al_2O_3). If the data in Table 2 are correlated as a unit, i.e., pH_{pzc} vs wt% of SiO_2 (for example), we find the "goodness of fit" correlation coefficient is 0.91. On the other hand, if we separately consider those composites formed on Al_2O_3 and on SiO_2 using the same basis (wt% SiO_2), we find correlation coefficients of 0.99 (SiO_2/Al_2O_3) and 0.98 (Al_2O_3/SiO_2). The "aqueous characterization" of this oxide family seems to favor differentiation based on the primary phase, while unique interpretation of the "gas-phase characterization" results is not as apparent.

TABLE 3

Raw Data from Potentiometric Titration at Background Ionic Strength = 0.07 *M* ($NaNO_3$)

Mass of acid/base	pH blank	pH with support[a]
	(a) Al_2O_3	
0.39	2.7	6.89
0.29	2.83	7.08
0.15	3.11	7.59
0.05	3.51	8.18
0.06	3.52	5.28
0.16	3.11	4.87
0.33	2.79	4.27
0.48	2.63	3.87
	(b) SiO_2	
0.33	2.95	2.76
0.15	3.26	3.07
0.0	5.62	4.26
0.16	3.27	8.40
0.39	2.90	7.11
0.47	2.81	6.47
0.64	2.69	6.01
0.84	2.57	5.65
1.01	2.50	5.39
1.22	2.42	5.08
1.37	2.37	4.93
	(c) 7% SiO_2/Al_2O_3	
0.35	2.75	4.83
0.20	2.99	5.28
0.12	3.21	5.73
0.03	3.73	6.18
0.07	10.53	6.63
0.17	10.92	7.08
0.25	11.1	7.53
0.35	11.23	7.97

[a] Support area/volume solution = 6.5×10^4 cm^{-1}.

Surface Charge

Table 3 provides the raw data needed for calculating the surface charge on a representative composite oxide, SiO_2, and Al_2O_3. The data for alumina and silica are included because another model, which we designate as the composite hydroxide model, requires the surface charge of the two pure phases. The data in Table 3 were analyzed by the procedures described in the Appendix. The

TABLE 4

pH-Dependent Surface Charge on Oxides at Ionic Strength = 0.07 *M*

pH	$\sigma_0(\mu c/cm^2)$
(a) Al_2O_3	
6.89	291.3
7.08	214.7
7.59	111.7
8.18	1.9
8.72	− 43.3
9.13	−112.0
9.73	−235.9
10.13	−358.7
(b) SiO_2	
2.76	1.27
3.07	0.55
4.26	− 0.10
5.6	− 2.19
6.89	− 5.21
7.53	− 6.38
7.99	− 8.51
8.35	− 11.23
8.61	− 13.35
8.92	− 16.09
9.07	− 18.08
9.24	− 20.43
9.41	− 23.66
(c) 7% SiO_2/Al_2O_3	
4.83	239.9
5.28	137.0
5.73	82.1
6.18	24.6
6.63	− 45.1
7.08	−111.3
7.53	−169.2
7.97	−229.4

surface charges vs pH data for these solids are given in Table 4. Note that these data are presented at an ionic strength = 0.07 *M;* they were interpolated from the 0.01 and 0.1 *M* potentiometric titration data. Theory predicts that, for an oxide that conforms to the simple model we use, at the pH = pzc, there will be a common crossing point for all potentiometric titration data, regardless of the ionic strength of the supporting electrolyte. However, the σ_0 vs pH result depends on ionic strength at all pH's $\neq$ pzc. In particular, our adsorption/impregnation experiments were conducted at an impregnant ionic strength = 0.07 *M*. Thus, σ_0 vs pH data are required at this ionic strength in order to assess the surface charge distribution of each support under the conditions prevailing during adsorption/impregnation.

Equilibrium Adsorbed Amounts

Table 5 presents the adsorption data for Pd(II) cations on Al_2O_3 and SiO_2 at a pH = 10.6 and electrolyte ionic strength of 0.07 *M*. From these data we conclude that the palladium complex is more strongly adsorbed on SiO_2 than Al_2O_3 in that very little compound could be detected in the wash from SiO_2 except at high concentrations. This was also found to be true for composites in which SiO_2 was the primary phase.

Adsorption isotherms for the pure supports and a representative composite are shown in Fig. 2. Table 6 summarizes the results of the adsorption/impregnation experiments. This table provides the saturation amounts at equilibrium. Silica adsorbs more than 20 times the amount adsorbed by Al_2O_3; the weight loading on SiO_2 corresponds to approximately 5%. When Al_2O_3 is the second phase, the amount adsorbed increases with increasing Al_2O_3 concentration; the increase is relatively small, however. When SiO_2 is the second phase, the amount adsorbed increases with increasing SiO_2 concentration; the increase in Pd complex adsorbed with concentration of this second phase is greater than that when Al_2O_3 is the second phase. Under the prevailing conditions, both SiO_2 and Al_2O_3 have net negative charges (pH > pH pzc). If this system conforms to the site-binding model, then the similarities/differences shown in Table 5 should be predictable on the basis of the net negative charge residing on the oxide(s) surface(s) at the prevailing conditions. Two models have been considered, and they and their predicted results are presented in the next section.

TABLE 5

Adsorption/Impregnation of Pd(II) on Pure Supports

(a) Al_2O_3

Initial concentration (mol/liter × 10^{+4})	Final concentration (mol/liter × 10^{+4})	Washed off (mol/g × 10^{7})	Adsorbed amount (mol/g × 10^{+6})
2.35	1.13	1.24	2.32
5.65	2.76	20.89	3.69
14.7	11.4	9.68	5.55
23.3	19.8	9.92	6.09
51.5	31.5	328.7	7.13
251.0	48	3990	7.07

(b) SiO_2

Initial concentration (mol/liter × 10^{+4})	Final concentration (mol/liter × 10^{+4})	Washed off (mol/g × 10^{8})	Adsorbed amount (mol/g × 10^{+5})
7.89	1.14	0	1.35
16.6	1.24	0	3.06
43.6	1.55	0	8.4
101.0	1.79	5.03	19.9
141.0	3.65	7.57	27.4
191.0	4.66	7.27	37.3
277.0	11.9	12.48	52.9
358.0	53.9	33.83	60.8
372.0	74.8	43.65	59.4

DISCUSSION

At the outset, it is important to recall several factors that were originally discussed in the Introduction. If we accept the hypothesis that this adsorption system conforms to the site-binding model and the fact that Pd $(NH_3)_4^{2+}$ is the dominant Pd(II) ion under the prevailing experimental conditions, then the following conclusion is reached. The confluence of theory and experiment comes with a comparison of the *calculated* charge structures on the oxides and the *experimentally* measured adsorption amounts of Pd(II). *These are determined by independent measurements.* In accordance with our adopting a simple diffuse model for the double layer, we would not expect quantitative agreement between calculated and measured quantities. However, if the basic chemistry of this system can be reasonably approximated by our hypotheses, then features which compare "calculated" with "measured" should provide semiquantitative agreement, provided experimental errors do not obscure either the calculated or measured quantities. Our analysis seeks to demonstrate that this assertion is valid.

The physical and chemical structure of composite oxides have been examined from several points of view. For example, Raman spectroscopy has been used extensively to characterize the physical structure of the second phase (*16–18*). Such techniques as XPS (*18*) and X-ray adsorption near-edge spectroscopy (*19*) have examined the chemical structure as well as provided data to confirm models related to geometrical structure. We have shown that additional information can be obtained by examining the properties of composite oxide when in contact with aqueous environments at various pHs and ionic strengths (*12, 13*). This approach potentially provides additional data on the properties of these carriers during catalyst preparation when they are used as supports for metals. Cobalt on MoO_3/Al_2O_3

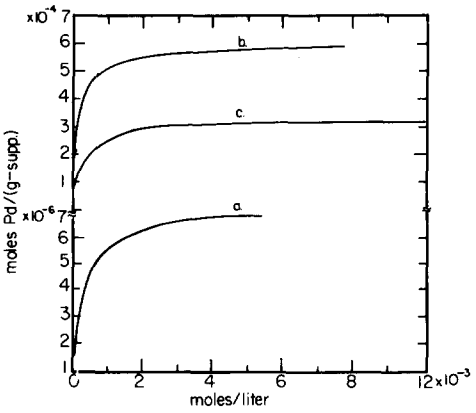

FIG. 2. Room temperature isotherms of $Pd(NH_3)_4^{2+}$ on Al_2O_3 (a), SiO_2 (b), and 3% Al_2O_3/SiO_2 (c) determined at pH = 10.6 and ionic strength = 0.07 *M*.

and Rh on CeO_2/Al_2O_3 are two such catalyst systems of great practical importance. If during catalyst preparation the metallic ions (Co, Rh, etc.) conform to an electrostatically driven adsorption, knowledge of the charge structure of the supporting oxides is of importance. As a first approximation, the pH-dependent charge development of the oxide(s) places restrictions/limitations on the adsorption/impregnation of metallic ions. It is this subject which is of interest here.

TABLE 6

Saturation Adsorption Amounts of Pd(II) at pH = 10.6, Ionic Strength = 0.07 *M*

Support	# Molecules of complex adsorbed/cm^2 × 10^{-13}[a]
Al_2O_3	0.24
3% Al_2O_3	4.8
7% Al_2O_3	5.4
10% Al_2O_3	5.5
3% SiO_2	1.5
7% SiO_2	2.7
10% SiO_2	3.9
SiO_2	5.6

[a] Based on measured BET surface area of each support.

Physical Structure

We have proposed that the variation in pzc of physical mixtures of pure oxides could serve as a "calibration curve" to evaluate the surface area of the individual phases of composite oxides (*12, 13*). This model assumes the pzc for a composite oxide to be the weighted sum, by surface area, of the pure oxide's pzc. A second model (*13*) has recently been presented to treat those cases when the concentration of the second-phase oxide is high (≥10–15%). This model considers the measured BET areas of the composites to be apportioned to each phase on the basis of their pzc and a calibration curve for physical mixtures. In light of the fact that the adsorption/impregnation studies of this work were confined to second-phase concentrations < 10%, we will only consider the originally proposed model. The parameters of this model are *N* and *d*, where *N* is the number of hemispherical clusters of the dispersed phase and *d* is the diameter of these clusters (Å). With the calibration curve (Fig. 1) and the pzc values of the composites (Table 2), we find the values of *d* and *N* and calculate the area contributed by the second phase. These results are presented in Table 7 for Al_2O_3/SiO_2 and SiO_2/Al_2O_3, respectively. The *N* and *d* values are quite similar in each set, however, the area contributed by the second phase does vary significantly for SiO_2/Al_2O_3, which is a consequence of the larger BET surface area of SiO_2 compared to Al_2O_3. The results given in Table 7 are further supported by the Pd^{2+} adsorbed amounts (Table 6).

Charge Structure of Composite Oxides

In the context of the simple diffuse layer model to characterize the surface charge development on oxide surfaces, the relevant parameters are the pzc and DPK. Their physical significance has been discussed in the Introduction. Operationally, one determines the net surface charge and fraction of charged and neutral sites directly from the

TABLE 7

Structural Properties of Composites Based on Model (Ref. (*12*))

%Al_2O_3 on SiO_2	pzc	(a) $N \times 10^{-19}$	d(Å)	Area of second phase (m^2/g)
1	3.40	1.7	9.54	24.45
3	3.79	5.7	9.2	76.08
7	3.94	2.2	16.86	96.87
10	4.09	1.9	19.78	118.01
%SiO_2 on Al_2O_3	pzc	(b) $N \times 10^{-20}$	d(Å)	Area of second phase (m^2/g)
3	7.29	1.4	8.90	169
7	6.39	1.8	10.86	324
10	5.37	4.1	9.22	545

potentiometric titration data. The model we use is that proposed by Gouy–Chapman, and a "user" friendly outline of the calculation steps is presented in the Appendix. We find that the range of pH values used (at fixed ionic strength) to determine the DPK is critical for an unambiguous set of results. Thus, we turn to the criterion proposed by Noh and Schwarz (*20*) to obtain a consistent set of DPK values for each support. Their earlier work concluded that utilization of data near the pH corresponding to the pzc of the oxide is necessary to estimate the intrinsic acidity constants. They proposed that the data within 3 pH units from the pzc toward pH = 7 be taken as the data base for consistent regression results.

Table 8 presents the values of pzc, DPK, N_S, the pH range used for each support, and the regression coefficient for the DPK over the given pH range. Values extracted from the literature for SiO_2 and Al_2O_3 are in good agreement with the results presented in Table 8. With these values in place, we can now turn to models proposed to represent the development of surface charge as a function of pH at a common ionic strength of 0.07 *M*.

Composite Hydroxyl Model

This model is a direct extension of the model described earlier and elsewhere (*12, 13*) which allows for an estimate of the properties of each phase of a composite oxide on the basis of the area contributed by each phase. Specifically, we assume that at fixed pH and ionic strength, each phase of the composite contributes positive, negative, and neutral sites in direct proportion to that phase's area contribution on the composite. The working equation which describes this hypothesis is given below.

In compact form, at the prevailing pH and ionic strength, we denote $\alpha_+, -, o$ as the fraction of positive, negative, or neutral sites. Then, for a given composite oxide, the total number of any type is

$$\left\{\frac{2\pi N\left(\frac{d}{2}\right)^2}{\left[\mathrm{SA} + \pi N\left(\frac{d}{2}\right)^2\right]}\right\}\{(\alpha_+, -, o)N_S\}_{S,P} + \left\{\frac{\left[\mathrm{SA} - \pi N\left(\frac{d}{2}\right)^2\right]}{\left[\mathrm{SA} + \pi N\left(\frac{d}{2}\right)^2\right]}\right\}\{(\alpha_+, -, o)N_S\}_{P,P},$$

where the first term uses the value of α and N_S associated with the second-phase oxide (S,P) and the second term uses parameters for the primary phase (P,P). The bracketed terms are the "weighting" coefficients determined from the structural model (*12, 13*), which provides an estimate of the surface area accessible for ion adsorption onto the second and primary phases of the composite, respectively. In the above, SA is the surface area (BET) of the primary phase and N and d are the parameters determined by the structural model described earlier (Table 7). For a given composite oxide system, the only "variable" in the expression is α, which depends on pH and ionic strength.

All quantities have been determined and, therefore, the charge distribution on the pure and composite oxides can be evaluated. The results are presented in Table 9. In this table, we also present the experimentally determined adsorbed amounts of the Pd(II) cations, remembering that each complex is

TABLE 8

Determination of Surface Ionization Parameters

Support	pzc	Regression pH range	DPK	N_S (sites/cm^2 × 10^{-15})	Regression coefficient	p$K1$	p$K2$
SiO_2	3.2	8.61–9.41	0.68	0.1	0.9367	2.86	3.54
10% SiO_2	5.37	6.04–7.21	2.90	1.2	0.9956	3.92	6.82
7% SiO_2	6.39	6.63–7.97	6.71	1.5	0.9961	3.03	9.74
3% SiO_2	7.29	7.17–8.40	8.79	1.1	0.9937	2.89	11.68
7% Al_2O_3	3.94	4.42–6.17	3.42	0.11	0.9971	2.23	5.65
3% Al_2O_3	3.79	4.61–6.73	3.05	0.11	0.9983	2.26	5.31
Al_2O_3	8.52	7.08–8.72	5.16	0.27	0.9843	5.94	11.10

divalent, thus each "consumes" two available negative sites. The amount adsorbed on each phase is also presented as well as the total number of neutral sites. We observe that the number of negative sites on SiO_2 is approximately the same as the number of divalent Pd(II) cations adsorbed. This suggests that the "efficiency" of the electrostatic interaction between charged species is quite good and may be due to the fact that we are only considering the strongly adsorbed Pd(II); the more weakly adsorbed would have been removed during the extensive (six times) water washing of the catalyst. This assertion is consistent with the observation that the number of negative sites on Al_2O_3 is greater than the Pd(II) adsorbed amount on this phase and the results presented in Table 5 which demonstrate that a considerable amount of complex is removed from Al_2O_3 during the washing.

Consider now the composites, their results are further represented in Fig. 3a to emphasize an important point. We note that the predicted and measured amounts are in reasonable agreement gven the simplicity of our modeling. However, the intercept is not zero as it should be. Based on the fact that adsorption on Al_2O_3 is weak compared to SiO_2, the washing step would remove complexes that "should" have been adsorbed on the negative sites. If these could be included in the inventory of adsorbed amount, the data point for Al_2O_3 (shaded circle) would be shifted to the right. Similar arguments can be made for the SiO_2/Al_2O_3 composites, but the "shift to the right" would become proportionally less as the SiO_2 load-

TABLE 9

Surface Concentration of Pd(II)—Composite Hydroxyl Model

Support	No. of complexes ads. × 10^{-13}/cm^2 (experimental)	No. of neg. sites × 10^{-13}/cm^2 (calculated)	No. of neg. sites on Al_2O_3 × 10^{-13}/cm^2 (calculated)	No. of neg. sites on SiO_2 × 10^{-13}/cm^2 (calculated)	Total neutral sites × 10^{-13}/cm^2 (calculated)
SiO_2	5.6	10	—	10	4 × 10^{-6}
3% Al_2O_3	4.8	9.1	0.22	8.9	2.8
7% Al_2O_3	5.4	8.9	0.28	8.6	3.5
10% Al_2O_3	5.5	8.7	0.33	8.3	4.2
10% SiO_2	3.9	6.7	0.81	5.9	10
7% SiO_2	2.7	5.2	1.20	4.0	15
3% SiO_2	1.5	3.9	1.50	2.3	19
Al_2O_3	0.24	2.0	2.00	—	25

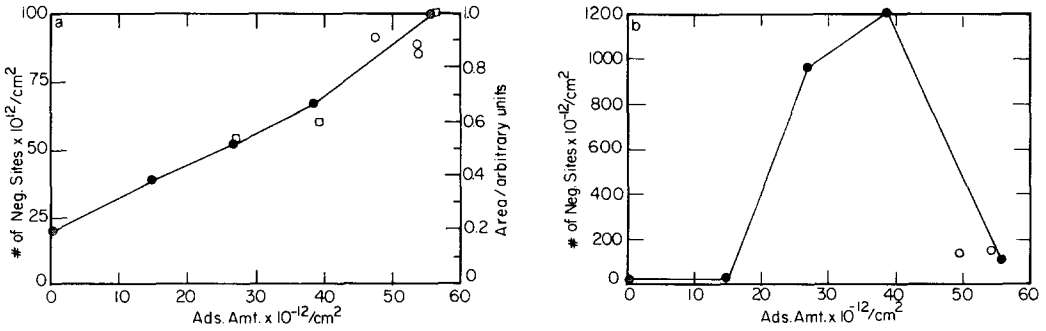

FIG. 3. Comparison of the calculated number of negative sites and the saturation adsorbed amount (strong bound) of Pd $(NH_3)_4^{2+}$ at a pH = 10.6 and ionic strength = 0.07 *M*. Key: ⊘ Al_2O_3 or SiO_2; ● SiO_2/Al_2O_3; ○ Al_2O_3/SiO_2. (a) Composite hydroxyl model (Also showing preliminary TPRd results [open squares, see text and Reference (*22*)]); (b) common hydroxyl model. Lines connecting points are for clarity.

ing increases due to its significant contribution of surface area (see Table 7b). The net effect would be a series of points that would more closely pass through the origin. From our data, it is not possible to quantify these assertions. However, to further support these arguments, we show later that the Langmuir adsorption constant is small for Pd^{2+}/Al_2O_3 interaction and, consequently, argue that the measured adsorbed amount of complex on Al_2O_3 is less than the predicted because the majority of the weakly bound electrostatic component is removed during the washing. Comparing the results for Al_2O_3/SiO_2 composites, the "spread" in calculated surface charge is smaller than in the former case. The scatter shown in Fig. 3a for these samples is likely due to experimental errors (difficult to evaluate).

Common Hydroxyl Model

Table 8 demonstrates that each support has its own N_S, DPK, and pzc. Therefore, we could treat the composite system as if it were a hypothetical oxide with the determined parameters. This was done, and we present the results in Table 10. Now the partitioning between each phase disappears, and all we can compare is the experimentally measured adsorbed amounts and the negative site concentration calculated assuming a common hydroxyl model. These results are shown in

TABLE 10

Surface Concentration of Pd(II)—Common Hydroxyl Model

Support	No. of complexes ads. × 10^{-13}/cm² (experimental)	No. of complexes ads. × 10^{-13}/cm² (calculated)	No. of neutral sites × 10^{-13}/cm² (calculated)
SiO_2	5.6	10	4×10^{-6}
3% Al_2O_3	4.8	11	2.3×10^{-4}
7% Al_2O_3	5.4	11	5×10^{-4}
10% Al_2O_3	5.5	—	—
10% SiO_2	3.9	120	0.032
7% SiO_2	2.7	96	53
3% SiO_2	1.5	2.2	110
Al_2O_3	0.24	2.0	25

Fig. 3b, where it can be seen that agreement is certainly poor compared to the composite hydroxyl model for the same composite series (Fig. 3a). We find that for the Al_2O_3/SiO_2 composites there is very little spread between the calculated adsorbed amounts. This is due to two factors. The negative surface charge on SiO_2 is much greater than it is on Al_2O_3 at pH 10.6 (see Table 4). Thus, the presence of SiO_2 as the primary phase would expect to dominate, with the second phase Al_2O_3 acting only as a perturbation during adsorption/impregnation. Of course the dominence of SiO_2 could be off-set if the second-phase Al_2O_3 contributed enough "surface area" on the composite. However, this is not the case (Table 7), and we find that both the common hydroxyl model and composite hydroxyl models give similar results. On the other hand, when Al_2O_3 is the primary phase, all factors stated above act in favor of adsorption on the SiO_2 component, and we can easily "resolve" the effects of increasing SiO_2 loading. It is important to remind the reader that ionic strength effects, which are significant at our electrolyte concentration and are contributing to suppression of Pd^{2+} adsorption on Al_2O_3, have been accounted for because the surface charge we determine from potentiometric titration data was at the same ionic strength as the adsorption/impregnation measurements. If there were some anomaly here, we would expect the adsorption results onto SiO_2 would also be affected, but they are not.

Additional insight of the adsorption properties of the oxides that comprise a composite can be obtained by analysis of the adsorption data. Adsorption data at constant pH obey the Langmuir isotherm

$$\frac{q}{S} = \frac{KC}{(1 + KC)},$$

where q (molecules/g cat.) is the adsorbed amount at equilibrium, S is the saturation capacity of the adsorbent, C is the equilibrium concentration in solution (mol/liter), and K is the so-called Langmuir constant (*9*). The basis for choosing this simple equation has been discussed elsewhere (*10, 21*).

We have examined the adsorption data of Pd(II) on the pure supports and find that this Langmuir isotherm well represents the data. The values of K for SiO_2 and Al_2O_3 are 6.8×10^3 lit/mol and 2.5×10^3 lit/mol, respectively, which is consistent with the previous conclusions that the Pd(II) complex is more strongly adsorbed on SiO_2 compared to Al_2O_3. Analysis of the adsorption of Pd(II) on the composite oxides (as shown in Fig. 2) requires some assumptions. It appears reasonable that if the Langmuir form is valid, then Pd(II) adsorption will occur on the Al_2O_3 and SiO_2 phases of the 3, 7, and 10% Al_2O_3/SiO_2 composites with Langmuir constants similar to those for each of the pure phases. However, the values of the saturation capacity will be a property of the alumina concentration on silica. Therefore, the total adsorbed Pd(II) complex on a composite would be

$$q_T = \frac{S_A K_A C}{1 + K_A C} + \frac{S_S K_S C}{1 + K_S C}$$

where S_A and S_S are the saturation amounts on Al_2O_3 and SiO_2 that comprise the composite; the values will depend upon the concentration of the second phase. The parameters K_A and K_S have been determined for the pure supports. Rearrangement of this "composite isotherm" and assuming that certain terms are small based on adsorption data from the pure supports, we arrive at the composite oxide isotherm,

$$q_T = (S_A + S_S)\frac{K_A K_S}{K_A + K_S} C \div \left(1 + \frac{K_A K_S}{K_A + K_S} C\right),$$

which is of the form in which an apparent Langmuir adsorption constant is expressed as $K_A K_S / K_A + K_S$. The apparent Langmuir constant was evaluated as (1.83×10^3 liter/mol), and the data for the 3, 7, and 10% Al_2O_3/SiO_2 composites were analyzed by least-squares analysis of the Langmuir function to

obtain the effective adsorption capacity of each composite. We found that the "fits" to these isotherms were of as good a quality as the fits to the isotherms for the pure phases (correlation coefficients between 0.98 and 0.99). While these results do not provide proof of the validity of our assumptions, they strongly suggest that each phase acts independent of the other, which is totally consistent with our overall assumptions that lead to the geometric and charge structure of this oxide system. The fact that the value of "K" for the composites is less than that for Al_2O_3 does not imply that the Pd(II) complex is less strongly adsorbed on these supports. Its value is simply a reflection of its "apparent" nature.

Finally, a part of a continuing study of this system, we have conducted preliminary temperature-programmed reduction (TPRd) studies of the dried precursors. The details are described elsewhere (*22*). We find that independent confirmation of the findings reached in this study is obtained from the TPRd results. Figure 3a also shows the hydrogen consumption attributed to the Pd(II) complex adsorbed on SiO_2/Al_2O_3 composites. The value for SiO_2 was normalized to the number of negative sites calculated for SiO_2, and the values for the composites were scaled to the H_2 consumption for Pd(II)/SiO_2. Peaks associated with the Al_2O_3 component were in the noise level for the composites. The agreement between theory and two independent experimental measurements (adsorption, TPRd) is almost quantitative.

CONCLUSIONS

We have shown at low loadings of a second-phase oxide on a primary oxide, the geometric and charge structure of the binary oxides can be modeled. Specifically, the adsorption/impregnation of Pd^{2+} precursors agrees with the surface concentration of available counter charge on a series of SiO_2/Al_2O_3 composite oxides at the prevailing pH and ionic strength of the impregnant.

Although it may be premature to put forth generalizations based solely on the results of this study, it appears a pH-directed selective adsorption onto a specific phase of a composite oxide can be achieved. The efficiency of the process improves when the catalytic metal ion complex conforms to the assumptions of an electrostatic interaction *and* when the adsorption interaction with the specific oxide phase is strong.

APPENDIX

The objective of this Appendix is to provide a "user frendly" recipe for evaluating the surface charge on an oxide from potentiometric titration data and the distribution of charge and potential for the Gouy–Chapman model. We find that although numerous texts discuss this problem, few provide a clear methodology for calculation (see Ref. (*14*, Chap. 10)).

The basic equation is

$$\sigma_O = F(\Gamma_{H+} - \Gamma_{OH-}) \qquad (1)$$

where

σ_O = surface charge, coulombs/cm^2
F = Faraday's constant = 96,487 coulombs/g-mol
$(\Gamma_{H+} - \Gamma_{OH+})$ = adsorption density, g-mol/cm^2.

The operational equation which relates measured quantities to σ_O is given as

$$\sigma_O = \frac{F}{A}\{\Delta M - [S - Z]\}, \qquad (2)$$

where the surface charge, σ_O, is positive for H^+ adsorption and negative for OH^- adsorption. The other terms are identified below:

$$\Delta M = NV_t$$
$$S = (V_e + V_t)\frac{10^{-a}}{\gamma_{soln}}$$
$$Z = V_e\frac{10^{-a_b}}{\gamma_{blank}}$$
$$A = W \cdot S_A \cdot 10^4$$
N = normality of HNO_3 or NaOH solution mol/lit

V_t = volume of titrant added, ml
V_e = volume of the electrolyte solution, ml
a = pH of the suspension of oxide for the added amount of acid, V_t ml of NHO_3 for titration with acid

or

a = 14- (pH of the suspension of oxide for the added amount of base, V_t ml of NaOH for titration with base)
a_b = pH of the electrolyte solution with oxide suspension in the absence of added acid

or

a_b = 14- (pH of the electrolyte solution with oxide suspension in the absence of added base
W = weight of oxide or composite oxide added, g
S_A = surface area of oxide or composite oxide, m^2/g
γ_{soln} = activity coefficient of the solution with oxide suspension
γ_{blank} = activity coefficient of the electrolyte solution with added acid or base without oxide suspension.

After the surface charge at each ionic strength is calculated, these values are plotted against the prevailing pH to determine the common intersection point which is the pzc. The Gouy–Chapman theory is then used to calculate the surface potential, χ_d. The relevant equations are

$$\sigma_O + \sigma_d = 0 \tag{3}$$

$$\sigma_d = -0.1174C^{1/2}\,\mathrm{Sinh}\left(\frac{ze\psi_d}{2kT}\right) \tag{4}$$

$$\sigma_0 = 0.1174C^{1/2}\,\mathrm{Sinh}\left(\frac{ze\psi_O}{2kT}\right) \quad \text{or} \tag{5}$$

$$\psi_O = \frac{2kT}{e}\,\mathrm{Sinh}^{-1}\left(\frac{\sigma_O}{0.1174C^{1/2}}\right) = \frac{2kT}{e}\ln(b + \sqrt{b^2+1}), \tag{6}$$

where

$b = \dfrac{\sigma_O}{0.1174C^{1/2}}$
σ_d = diffuse layer charge, microcouloubs/cm^2
C = bulk concentration, mol/lit
z = charge of the supporting electrolyte counterion in the diffuse layer
ψ_O = potential between surface and solution, volts.

The traditional Nernst potential, χ_N, is a useful concept. It is used as an operational parameter to relate the hydrogen concentration to the pzc.

The Nernst potential, ψ_N can be written as

$$\psi_N = \frac{kT}{e}\ln\left(\frac{[H_b^+]}{[H_b^+]_{pzc}}\right). \tag{7}$$

The following parameters are defined:

$$y_N = \frac{e\psi_N}{kT} = \ln\left(\frac{[H_b^+]}{[H_b^+]_{pzc}}\right) \tag{8}$$

and $y_O = e\psi_O/kT$. (9)

The intrinsic acidity constants for protonation (K_1) and deprotonation (K_2) are combined to form

$$\delta = 2\left(\frac{K_2}{K_1}\right)^{1/2}. \tag{10}$$

The fractional surface charge based on the total number of ionizable sites, N_S (sites/cm^2) is

$$\alpha = \frac{\sigma_O}{eN_S} \tag{11}$$

which can be written as

$$\alpha = \frac{\sigma_O}{eN_S} = \frac{\delta\,\mathrm{Sinh}(y_N - y_O)}{1 + \delta\,\mathrm{Cosh}(y_N - y_O)} \tag{12}$$

and rearranged as

$$\mathrm{Cosh}(y_N - y_O) = eN_S\frac{\delta\,\mathrm{Sinh}(y_N - y_O)}{\sigma_O} - \frac{1}{\delta}. \tag{13}$$

Defining

$$X = \frac{\mathrm{Sinh}(y_N - y_O)}{\sigma_O} \quad (14)$$

$$Y = \mathrm{Cosh}(y_N - y_O) \quad (15)$$

From bulk pH values recorded during the titration and the pzc, y_N, and y_O are evaluated. Finally, from a plot of Y vs X (Eq. 13)), we can calculate the total number of sites, N_S, DPK, and hence K_1 and K_2 from the slope and intercept.
Therefore,

$$\delta = 2\left(\frac{K_2}{K_1}\right)^{1/2} = -\frac{1}{\text{intercept}} \quad (16)$$

$$\mathrm{DPK} = \mathrm{p}K_2 - \mathrm{p}K_1 = -2\log\left(\frac{-0.5}{\text{intercept}}\right) \quad (17)$$

$$N_S = \frac{\text{slope}}{e}. \quad (18)$$

ACKNOWLEDGMENTS

This work was supported by NSF under Grant CBT-8900514.

REFERENCES

1. Brunelle, J. P., *Pure Appl. Chem.* **50,** 1211 (1978).
2. Che, M., and Bonneviet, L., *Pure Appl. Chem.* **60,** 1369 (1988).
3. Hohl, H., and Stumm, W. J., *J. Colloid Interface Sci.* **55,** 281 (1976).
4. Stumm, W., Huang, C. P., and Jenkins, S. R., *Crom Chim. Acta* **42,** 223 (1970).
5. Bowden, J. W., Posner, A. M., and Quirk, J. P., *Aust. J. Soil Res.* **15,** 121 (1977).
6. Davis, J. A., James, R. O., and Leckie, J. O., *J. Colloid Interface Sci.* **63,** 480 (1978).
7. Noh, J. S., and Schwarz, J. A., *J. Catal.* **127,** 22 (1991).
8. Contescu, C., Sivaraj, C., Schwarz, J. A., *Appl. Catal.* **74,** 95 (1991).
9. Contescu, C., and Vass, M. I., *Appl. Catal.* **33,** 259 (1987).
10. Sivaraj, C., Contescu, C., and Schwarz, J. A., *J. Catal.* **132,** 422 (1991).
11. Zhang, R., Schwarz, J. A., Dayte, A., and Baltrus, J. P., submitted for publication.
12. Subramanian, S., Noh, J. S., and Schwarz, J. A., *J. Catal.* **114,** 433 (1988).
13. Brady, R. L., Southmayd, D., Contescu, C., Zhang, R., and Schwarz, J. A., *J. Catal.* **129,** 195 (1991).
14. Stumm, W., and Morgan, J. J., "Aquatic Chemistry," 2nd ed., p. 632. Wiley, New York 1981.
15. Noh, J. S., and Schwarz, J. A., *J. Colloid Interface Sci.* **130,** 157 (1989).
16. Ng, K. T., and Hercules, D. M., *J. Phys. Chem.* **80,** 2094 (1976).
17. Salvati, L., Jr., Makovsky, L. E., Stencel, J. M., Brown, F. R., and Hercules, D. M., *J. Phys. Chem.* **85,** 3700 (1981).
18. Stencel, J. M., Makosky, L. E., Diehl, J. K., and Sarkas, T. H., *Raman Spectrosc. Lett.* **15,** 282 (1984).
19. Horsley, J. A., Wachs, I. E., Brown, J. M., Via, G. H., and Hardcastle, F. D., *J. Phys. Chem.* **91,** 4014 (1987).
20. Noh, J. S., and Schwarz, J. A., *J. Colloid Interface Sci.* **139,** 139 (1990).
21. Weisz, P. B., *Trans. Faraday Soc.* **63,** 1801 (1967).
22. Ugbor, C. T., Masters Thesis, Chemical Engineering and Materials Science Dept., Syracuse University, 1992.